Journal of Physics: Conference Series

PAPER • OPEN ACCESS

Analysis of the CMD-3 detector data: selection of low-energy electron-positron annihilation into $KK\pi\pi^0$

To cite this article: A A Uskov 2023 *J. Phys.: Conf. Ser.* **2438** 012069


Analysis of the CMD-3 detector data: selection of low-energy electron-positron annihilation into KKππ⁰

A A Uskov[1]

1. Budker Institute of Nuclear Physics, Novosibirsk, Russia

a.uskov+conferences@alumni.nsu.ru

Abstract. We explore the process $e^+e^- \to K_S K^{+-}\pi^{-+}\pi^0$ with the CMD-3 detector at the electron-positron collider VEPP-2000. Here, we present a selection algorithm. The data amassed by the CMD-3 detector in the energy range of 1.2–2 GeV during 2011, 2012, 2017, 2019 runs, with a total luminosity integral of ~120pb^{-1} backs the analysis. Two reasons stand behind the study. First, a recent report of anomalous magnetic moment discrepancy broadening to 4.2σ, see Fermilab article [1]. Searching for New Physics demand sharper Hadronic Vacuum Polarization (HVP) estimate. In its turn, HVP computation relies heavily on hadronic cross-sections measurement. Second, an intermediate vector resonance near 2 GeV (ϕ'') is still a mystery. It might be a $s\bar{s}$ state, or a hybrid $s\bar{s}g$, or $\Lambda\bar{\Lambda}$ state. Untangling partial decay widths, measuring isospin 1 and 0 cross-sections for $e^+e^- \to K_S K^{+-}\pi^{-+}\pi^0$, might discern between different ϕ'' models.

1. Introduction

Hadronic cross-sections in the energy region below 2 GeV present several opportunities:

First, they account for more than 90% of the theoretical value of hadronic vacuum polarization (HVP). Recently, anomalous magnetic moment discrepancy was reported to broaden to 4.2σ [1]. So, searches for New Physics demand sharper HVP estimate. In its turn, HVP computation boils down to using measured hadronic cross-sections.

Second, this energy region below 2 GeV is non-perturbative QCD regime. Such regime reveals rich intermediate dynamics of hadronization. In the Vector Meson Dominance (VMD) framework, the hadronization dynamics can be described by $J^{PC} = 1^{--}$ resonances like ρ, ω, ϕ. Only first excitations are studied well. Yet, some further states like intermediate vector resonance near 2 GeV (ϕ'') are still a mystery. This resonance might be a $s\bar{s}$ state, or a hybrid $s\bar{s}g$, or $\Lambda\bar{\Lambda}$ state [2]. If one untangles partial decay widths, and finds isospin 1 and 0 cross-sections for $e^+e^- \to K_S K^{+-}\pi^{-+}\pi^0$, it might help to discern between different ϕ'' models.

Journal of Physics: Conference Series **2438** (2023) 012069 doi:10.1088/1742-6596/2438/1/012069

In this article, we explore the process $e^+e^- \to K_S K^{+-} \pi^{-+} \pi^0$ with the CMD-3 detector at the electron-positron collider VEPP-2000. Here, we present a selection algorithm for this process. The data amassed by the CMD-3 detector in the energy range of 1.2−2 GeV during the 2011, 2012, 2017, 2019 runs, with a total luminosity integral of ~120pb^{-1} backs the analysis. We selected 4762 events of $e^+e^- \to K_S K^{+-} \pi^{-+} \pi^0$. The proposed algorithm consists of 6 stages:

1. Select high-quality tracks traversing the sensitive region of the drift chamber.
2. Find K_S via kinematic reconstruction and apply K_S decay length cut.
3. Apply kinematic fit χ^2 cut. In signal hypothesis ($K_S K^{+-} \pi^{-+} \pi^0$), four charged tracks, and one missing π^0 are included. In this step, we try several background hypotheses as well: $K_S K^{+-} \pi^{-+}$, 5π, $K^+K^-\pi^+\pi^-$.
4. Select a suitable 2D region on ΔE:ΔP, optimized by MC.
5. Apply dE/dx particle identification. Suppress background where no charged K found.
6. Subtract resonant background known from known relative cross-sections and MC. Remove non-resonant background by sidebands.

We apply the same algorithm to full Monte Carlo simulation of detector. Multi-hadronic generator (MHG-2000) made by CMD-3 team [6], shows agreement with experiment. Being data-driven, it includes relative cross-sections from experiment. So, it allows to stratify background by final states. The selection background subtraction method satisfies the requirement of less than 1% of systematic uncertainty.

2. Pre-selection

The $e^+e^- \to K_S K^{+-} \pi^{-+} \pi^0$ process event has four charged tracks. Each of the tracks is detected by the CMD-3 detector drift chamber (DC). The DC is filled with 80:20 argon-isobutane mixture and submerged into 1.3 T magnetic field. Table 1 summarizes the selection of high-quality tracks in the sensitive region of the chamber.

Table 1. Track-based pre-selection criteria.

Selection type	Selection criteria
Polar angle	$1 < \Theta_{tr} < \pi - 1$
Number of hits per track	> 10
Track momentum	60 MeV to 800 MeV
Track z	< 12 cm
Track (not from K_S) impact parameter	> 0.1 cm

The particles K^{+-} and π^{-+} fly directly out of the beam interaction point (IP), while the K_S has a decay length of a 1 cm scale. The reconstruction of K_S displaced vertex helps to achieve 10 times less background. The particle K_S was detected in $K_S \to \pi^+ \pi^-$ mode. As we show later, most of the background stems from the $e^+e^- \to 4\pi$ process. This background process does not involve the K_S. So, if a K_S was reconstructed from two π particles from the events of $e^+e^- \to 4\pi$, this K_S would be fake. By simulation we know that this fake K_S does not actually travel any distance before decay. That's why, the selection cut by K_S decay length noticeably reduced the background [3].

We use kinematic reconstruction [4, 5] not only to find the K_S vertex, but also to filter signal based on its χ^2. As usual, tracks are varied within their experimental error matrices. Lagrange multiplier enforces the energy-momentum conservation law. The signal hypothesis includes the right mass for each of the particles. Every combination was tried, and only the one with the least χ^2 was taken. In the signal hypothesis we assume a missing particle with a mass of π^0 and momentum equal to the sum of all detected particle momentums. Table 2 demonstrates K_S selection criteria.

Table 2. Event level selection criteria.

Selection type	Selection criteria
K_S found by kinematic fit	= 1
K_S decay length	> 0.5 cm
Tracks from IP	= 2
Track from K_S	= 2
χ^2 ($K_S K^{+-} \pi^{-+} \pi^0$)	< 150
Tracks charges at vertices	opposite

3. A map of background processes

In e^+e^- collisions several hadronic processes happen at once. Some of them could mimic the detector signature of the signal. To see all different background clusters, we built a special 2D-plot called ΔE:ΔP, where ΔP is momentum imbalance = $|p_1 + p_2 + p_3 + p_4|$ and ΔE is energy imbalance. The value of ΔE is equal to the value of the total energy minus double value of the beam energy. The mass in $E^2 - p^2 = m^2_\pi$ was taken equal to the mass of the π particle. That's why, by energy conservation, events of $e^+e^- \to 4\pi$ collect near (ΔE, ΔP) = 0. If other processes are considered, they collect near a shifted value of ΔE. The explanation of this shift is that when the mass of K is underestimated by the mass of π, the cluster shifts down. For example, the cluster for the process $e^+e^- \to K_S K^{+-} \pi^{-+}$ is shifted to $\Delta E = -200$.

When a particle with a noticeable momentum is missing the cluster for such events on ΔE: ΔP gathers around non-zero ΔP. In Fig. 1, one might see such events with non-zero ΔP: the events of $e^+e^- \to 4\pi + \pi^0$, $e^+e^- \to 4\pi + 2\pi^0$, $e^+e^- \to K_S \pi^+ \pi^- + K_L$, and the signal $e^+e^- \to K_S K^{+-} \pi^{-+} \pi^0$. The clusters for different processes partially overlap. Another feature of this plot – radiative tails. When ISR photon gets emitted one can see a line at 45 degrees. This line is called a radiative tail. Tails explain why events of the process $e^+e^- \to K_S K^{+-} \pi^{-+}$ partially get into the $e^+e^- \to K_S K^{+-} \pi^{-+} \pi^0$ signal region on ΔE: ΔP.

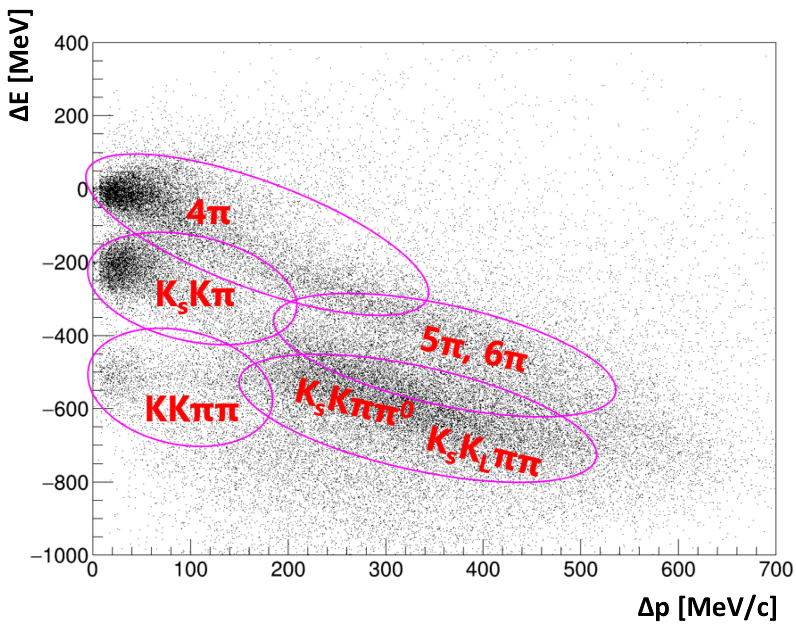

Figure 1. Experimental ΔE: ΔP 2D-distribution is shown. Different process clusters are highlighted. Those cluster positions were determined by multi-hadron generator MHG-2000. Boundaries are shown roughly because many clusters overlap a lot.

4. Selection of the signal process. The procedure of event counting.

The K_S invariant mass shown in Fig. 2 was used to count signal events. Two types of background exist: resonant and uniform. The resonant background is defined to have a peak in K_S invariant mass distribution located near the on-shell mass of K_S. The uniform background is defined to have no peak. Therefore, uniform background can be easily subtracted with the sideband method. Yet, it might be more difficult to identify and subtract the resonant background. In this paper. we wanted to achieve a less than 1% systematic uncertainty of the background subtraction procedure. Therefore, we applied an additional step. First, the resonant background must be minimized. It was minimized to be less than 10%. Second, the number of residual events of the resonant background must be estimated and subtracted. It was estimated from the MHG-2000 multi-hadron simulation. The relative cross-sections of the background processes, included in the simulation, are known with better than 10% precision. If a 10% value is known with 10% precision, that is only 10% · 10% = 1% contribution to the total systematic uncertainty. In this way, the resonant part of the background was reasonably suppressed. Indeed, when the total systematic uncertainty of the $e^+e^- \to K_S K^{+-} \pi^{-+} \pi^0$ cross-section measurement is calculated, other uncertainties dominate.

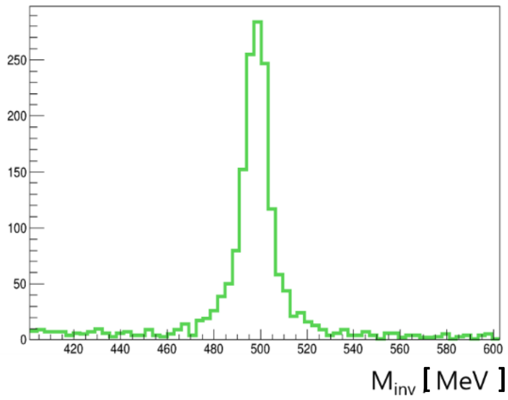

Figure 2. The K_S invariant mass distribution after all kinematic cuts is shown. This distribution was used to count signal events.

After the stages of tracks pre-selection, kinematic reconstruction, K_S decay length selection, and ΔE:ΔP region cut, the MHG-2000 simulation provided the composition of physical background by exclusive final states shown in Fig. 3. In this figure, non-resonant background is 5π and 6π. It appeared that the main resonant background – $K_SK_L\pi^+\pi^-$ accounted for 14 % of all events. Without the final stage of our selection algorithm, the systematic precision did not meet 1% requirement.

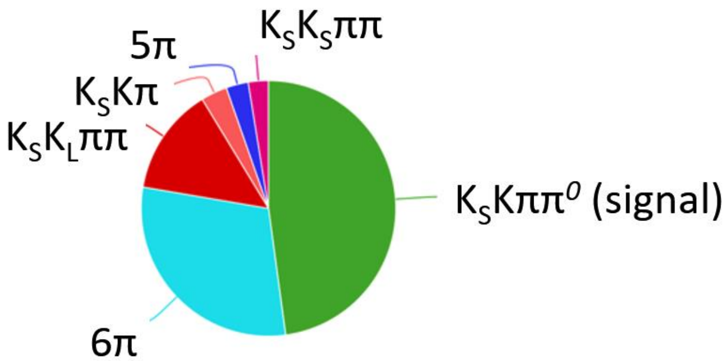

Figure 3. A pie chart shows relative background composition by final states. All cuts except for the dE/dx cut were applied. The relative number of events was obtained by MHG-2000 Monte Carlo simulation.

To fight this issue, note that the main resonant background – $e^+e^- \rightarrow K_SK_L\pi^+\pi^-$ has two charged pions instead of $K^{+-}\pi^{-+}$ in signal process $e^+e^- \rightarrow K_SK^{+-}\pi^{-+}\pi^0$. We harness dE/dx likelihood function [7, 8] to tell apart kaons and pions. As one can see in Fig. 4, dE/dx suppresion changes the background composition. Now resonant background consists of $K_SK_L\pi^+\pi^-$ for only 3% and $K_SK^{+-}\pi^{-+}$ for 5%. Both of them are known with a good precision for example from [3, 9]

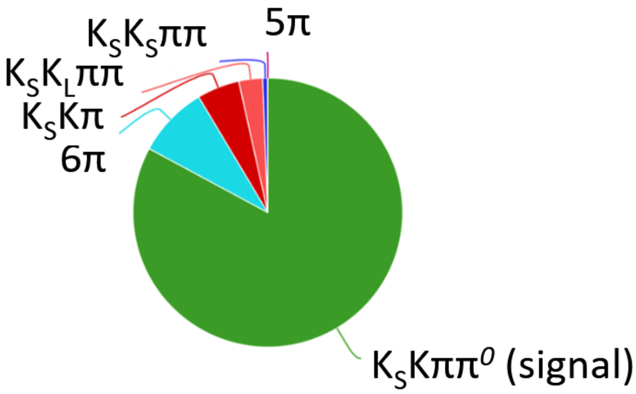

Figure 4. A pie chart shows relative background composition by final states. All cuts including the dE/dx cut were applied. The relative number of events was obtained by MHG-2000 Monte Carlo simulation.

As a result, our selection algorithm, in particular its background subtraction part, satisfies the requirement of less than 1% of systematic uncertainty.

5. Conclusion

In this paper, we selected 4762 events of $e^+e^- \rightarrow K_SK^{+-}\pi^{-+}\pi^0$ with the CMD-3 detector on the VEPP-2000 collider in the region of energies less than 2 GeV. The proposed algorithm meets the requirement for the systematic uncertainty caused by background subtraction to be less than 1%.

The process has rich intermediate dynamics [10]. So, by analysing partial decay widths, we might glean insight into ϕ'' composition [11, 12, 13]. The data obtained is to be used in $(g\text{-}2)_\mu$ HVP contribution calculation.

References:

[1] Abi B, et al. (Muon g−2 Collaboration) 2021 *Phys. Rev. Lett.* **126.14** 141801
[2] Ablikim M, Phys. Rev. Lett. **124** 112001 (2020)
[3] Uskov A A, et al. 2020 Phys. Scr. **95** 104002
[4] Gribanov S S, KFCmd: CMD-3 kinematic fitter https://github.com/sergeigribanov/KFCmd

[5] Grivanov S S, et al. 2020 J. High Energ. Phys. **112**
[6] Korobov A A, Journal of Physics: Conference Series 1525, 012019
[7] Ivanov V L, et al. *Nucl.Instrum.Meth.A* 1015 (2021) 165761
[8] Shemyakin D N, et al. 2016 Physics Letters B**756** 153-160
[9] Aubert B, et al. 2008 Phys. Rev. D **77** 092002
[10] Lees J P, et al. 2017 Physical Review D 95.9
[11] Ablikim M, et al. 2020 Chinese Physics C 44 4 040001
[12] Qi Li, et.al 2021 Chinese Physics C 45 2 023116
[13] Pei-Lian Liu, et.al 2015 Chinese Physics C 39 8 082001